ACS Chemical Neuroscience

Research Article

pubs.acs.org/chemneuro

Endocannabinoid Enzyme Engineering: Soluble Human Thio-Monoacylglycerol Lipase (sol-S-hMGL)

Ioannis Karageorgos,[†] Nikolai Zvonok,[†] David R. Janero,*[,†] V. Kiran Vemuri,[†] Vidyanand Shukla,[†] Thomas E. Wales,[‡] John R. Engen,[‡] and Alexandros Makriyannis*[,†]

[†]Center for Drug Discovery and [‡]Department of Chemistry and Chemical Biology and Barnett Institute of Chemical and Biological Analysis, Northeastern University, Boston, Massachusetts 02115-5000, United States

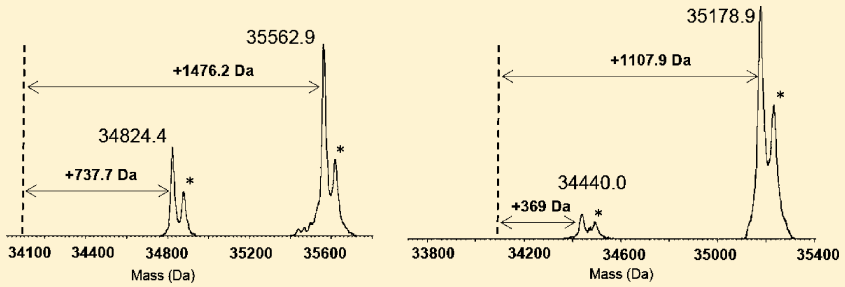

ABSTRACT: In the mammalian central nervous system, monoacylglycerol lipase (MGL) is principally responsible for inactivating the endocannabinoid signaling lipid 2-arachidonoylglycerol (2-AG) and modulates cannabinoid-1 receptor (CB1R) desensitization and signal intensity. MGL is also a drug target for diseases in which CB1R stimulation may be therapeutic. To inform the design of human MGL (hMGL) inhibitors, we have engineered a Leu(Leu^{169};Leu^{176})-to-Ser(Ser^{169};Ser^{176}) double hMGL mutant (sol-hMGL) which exhibited enhanced solubility properties, and we further mutated this variant by substituting its catalytic-triad Ser^{122} with Cys (sol-S-hMGL). The hMGL variants hydrolyzed both 2-AG and a fluorogenic reporter substrate with comparable affinities. Our results suggest that the hMGL cysteine mutant maintains the same overall architecture as wild-type hMGL. The results also underscore the superior nucleophilic nature of the reactive catalytic Ser^{122} residue as compared to that of Cys^{122} in the sol-S-hMGL mutant and suggest that the nucleophilic character of the Cys^{122} residue is not commensurately enhanced within the three dimensional architecture of hMGL. The interaction of the sol-hMGL variants with the irreversible inhibitors AM6580 and *N*-arachidonylmaleimide (NAM) and the reversible inhibitor AM10212 was profiled. LC/MS analysis of tryptic digests from sol-S-hMGL directly demonstrate covalent modification of this variant by NAM and AM6580, consistent with enzyme thiol alkylation and carbamoylation, respectively. These data provide insight into hMGL catalysis, the key role of the nucleophilic character of Ser^{122}, and the mechanisms underlying hMGL inhibition by different classes of small molecules.

KEYWORDS: *Active site, catalytic mechanism, drug design, enzyme inhibition, serine hydrolase*

The endocannabinoid system is a cellular signaling network in which serine hydrolase enzymes exert critical control over the tissue tone of endogenous lipid ligands (endocannabinoids) that engage and activate cannabinoid receptors.[1] In the central nervous system (CNS), monoacylglycerol lipase (MGL) is the endocannabinoid-system enzyme primarily (~85%) responsible for inactivating the endocannabinoid 2-arachidonoylglycerol (2-AG), a full agonist at both principal seven-transmembrane cannabinoid receptors, cannabinoid-1 (CB1R) and cannabinoid-2 (CB2R). Since 2-AG is a key endocannabinoid in the CNS where CB1R is primarily localized, MGL activity is a critical modulator of central, 2-AG tone and CB1R signaling intensity to influence such processes as learning and memory.[2−6] By acting on 2-AG in the brain, MGL also regulates substrate pools of arachidonic acid for the cyclooxygenase-mediated biosynthesis of proinflammatory prostaglandins.[7] Fatty-acid products generated from the hydrolytic action of MGL on various monoglycerides control a free fatty-acid network encompassing several oncogenic signaling lipids that promote features of the malignant cellular phenotype (migration, invasion) as well as aggressive tumor growth in vivo.[8,9] These data suggest that targeted MGL inhibitors may have therapeutic potential in neuroinflammatory diseases and cancer. Furthermore, acute MGL inhibition with a selective inhibitor, JZL184, elevates CNS 2-AG levels and elicits CB1R-dependent hypomotility and analgesia, suggesting the attractiveness of MGL inhibition for treating (neuropathic) pain.[10] Genetic MGL ablation in mice compromises the associated analgesic activity, as does chronic pharmacological MGL inhibition leading to receptor desensitization, indicating that

Special Issue: Therapeutic Potential of Endocannabinoid Metabolic Enzymes

Received: February 22, 2012
Accepted: March 20, 2012
Published: March 20, 2012

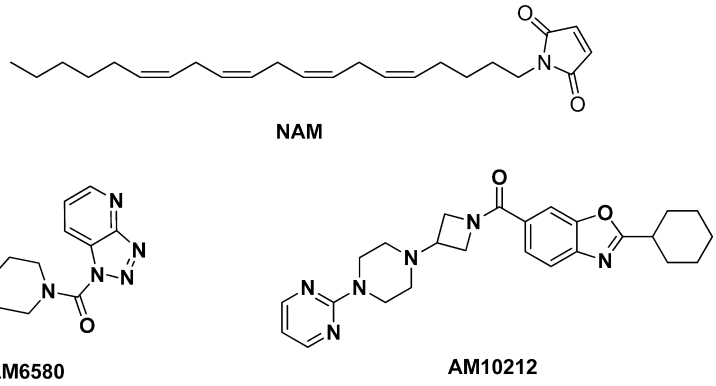

Figure 1. Chemical structures of NAM, AM6580, and AM10212.

temporal tuning of MGL inhibitors represents an important criterion for their druggability.[4,5]

Like the majority of metabolic serine hydrolases, MGL exhibits the canonical α/β-hydrolase fold and a flexible regulatory lid, a domain that may be involved in MGL membrane anchoring.[11,12] Analyses of recently obtained crystal structures suggest that two distinct human MGL (hMGL) conformational states exist in equilibrium. The first, a more hydrophilic state with a closed lid, accommodates native 2-AG substrate or bound reversible inhibitor, whereas the second, more hydrophobic and with an open lid, represents *apo*-hMGL and hMGL covalently modified by the irreversible inhibitor, SAR629.[13−15] A model of hMGL interaction with 2-AG substrate has been proposed in which the enzyme undergoes conformational and electrostatic changes during the catalytic cycle, ultimately resulting in its dissociation from the membrane upon cycle completion.[15] (h)MGL also displays the classic serine (Ser^{122})-histidine (His^{269})-aspartic acid (Asp^{239}) catalytic triad typical of most serine hydrolases.[11,12,16] In the first step of the catalytic cycle, a hydroxyl group of Ser^{122} is activated by a proton relay involving the basic His^{269} and acidic Asp^{239} residues, and the activated Ser^{122} nucleophile attacks the carbonyl group of 2-AG, forming an acyl-enzyme intermediate as initial reaction product via covalent tetrahedral enzyme−substrate transition state 1. The second step involves the His^{269}-facilitated hydrolysis of the acyl-enzyme intermediate via tetrahedral covalent enzyme−substrate transition state 2, resulting in formation of final reaction product and active regenerated enzyme. In aggregate, these high-resolution structural and molecular enzymology data suggest that the activated Ser^{122} nucleophile of the (h)MGL catalytic triad is critical to both the enzyme's catalytic mechanism and the structural and topological dynamics associated with the (h)MGL catalytic cycle. This suggestion has gained direct experimental support from studies in our laboratory involving mass spectroscopy (MS) characterization of hMGL and its inhibition by various covalent inhibitors,[17,18] functional hMGL mutagenesis,[18] and identification by nuclear magnetic resonance spectroscopy (NMR) of a dynamic, active-site hydrogen-bond network.[19]

Although crystal structures of hMGL in *apo* and enzyme-ligand forms are available, questions remain concerning the structural and dynamic details associated with the opening and closing of the enzyme's lid domain, the process of enzyme-membrane (dis)association, and the interaction profiles of small-molecule inhibitors. We and others have engineered assorted recombinant hMGL deletion mutants as well as single, double, and triple point mutants in order to increase expression yield, enhance enzyme aqueous solubility, and probe the structural basis of hMGL catalysis/inhibition.[15,17,18] In the present work, we have employed site-directed mutagenesis and targeted ligand synthesis as a molecular-pharmacology approach for gaining further insight into the mechanism of hMGL catalysis and the molecular features involved in reversible and irreversible hMGL inactivation by inhibitors. In order to enhance hMGL solubility, we constructed a Leu-(Leu^{169};Leu^{176})-to-Ser(Ser^{169};Ser^{176}), 2L/2S double hMGL mutant (sol-hMGL). This more soluble form of wild-type hMGL was further engineered by mutating Ser^{122} in the catalytic triad to Cys, a triple mutant hMGL variant designated as sol-S-hMGL. The aim of this study is to compare the biochemical characteristics of the engineered Cys^{122} hMGL variant with its corresponding Ser^{122} congener. Subsequently, we profiled the interaction of these two enzymes, whose only difference is the substitution of the catalytic Ser with a related amino acid nucleophile, with three mechanistically different inhibitors: the irreversible alkylating agent 1-((5*Z*,8*Z*,11*Z*,14*Z*)-icosa-5,8,11,14-tetraen-1-yl)-1H-pyrrole-2,5-dione (*N*-arachidonylmaleimide) (NAM),[18] the irreversible inhibitor [4-(9H-fluoren-9-yl)piperazin-1-yl][1,2,3]triazolo[4,5-b]pyridin-1-yl-methanone (AM6580),[20] and the reversible inhibitor 2-cyclohexyl-6-{[3-(4-pyrimidin-2-yl-piperazin-1-yl)azetidin-1-yl]carbonyl}-1,3-benzoxazole (AM10212)[21] (Figure 1). The resulting data inform the design of later-generation, hMGL-selective inhibitors as potential medicines.

RESULTS AND DISCUSSION

Expression, Purification, and Biochemical Characterization of hMGL Variants. We previously overexpressed functional hMGL in *E. coli*, purified the enzyme, and characterized its catalytic properties with the substrates 2-AG and arachidonoyl, 7-hydroxy-6-methoxy-4-methylcoumarin ester (AHMMCE).[18] We also obtained evidence for the involvement of Ser^{122} carbamoylation in wild-type hMGL inactivation by the acutely irreversible, active site-directed inhibitor, AM6701.[18,19] To enhance hMGL solubility and stability, we adopted an approach similar to that of Schalk-Hihi et al.[15] and introduced 2L/2S mutations into the enzyme to engineer the hMGL variant designated sol-hMGL. A further Ser^{122}-to-Cys substitution was also made, resulting in a triple mutant variant, sol-S-hMGL, that expressed exclusively in soluble form and at greater levels than had other hMGL mutants we generated previously.[18,19] By virtue of their 6-His tags, purification of both sol-hMGL and sol-S-hMGL could be

achieved by metal affinity-based chromatography, as evidenced by SDS-PAGE (Figure 2).

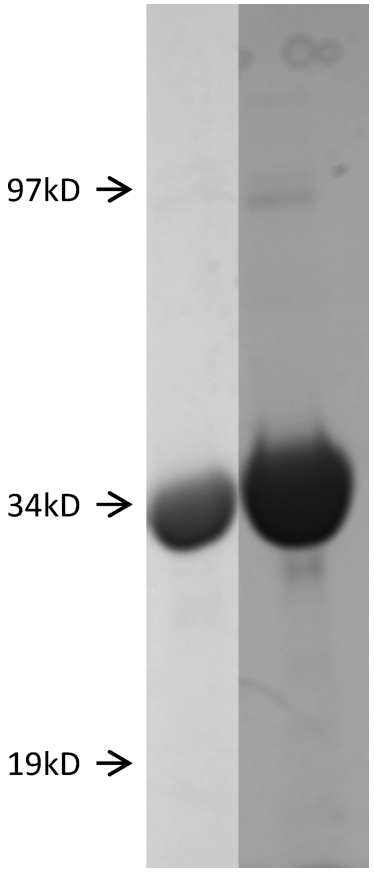

Figure 2. Coomassie-stained SDS-PAGE gels of purified, 6-His-tagged sol-hMGL (left lane) and sol-S-hMGL (right lane). Molecular masses are designated to the left of the gels.

Both sol-hMGL and sol-S-hMGL hydrolyzed endogenous 2-AG substrate and reporter fluorogenic substrate, AHMMCE (Table 1). These soluble hMGL variants evidenced comparable

Table 1. Apparent Kinetic Parameters with the Natural Substrate (2-AG) or the Model Fluorogenic Reporter Substrate, AHMMCE, for Purified Recombinant 6-His-tagged sol-hMGL and sol-S-hMGL Overexpressed in *E.coli*

	substrate			
	2-AG		AHMMCE	
enzyme	K_m (μM)	V_{max} (μM/min/μg)	K_m (μM)	V_{max} (μM/min/μg)
sol-hMGL	80	7.7	4.3	1068
sol-S-hMGL	69	0.1	16.0	75

(micromolar) affinities for 2-AG. The ~4-fold lower K_m of sol-hMGL vs sol-S-hMGL for AHMMCE suggests that substitution of the catalytic Ser^{122} with Cys marginally reduced the enzyme's affinity for this substrate (Table 1). However, substitution of the sol-hMGL catalytic Ser^{122} with Cys markedly reduced enzyme velocity with respect to that of sol-hMGL, a difference likely reflective of a reduced nucleophilic ability of the Cys^{122} in sol-S-hMGL vs the activated Ser^{122} in sol-hMGL. Although the soluble variants evidenced similar micromolar affinities for both 2-AG and AHMMCE as compared to wild-type hMGL, sol-hMGL hydrolyzed 2-AG and AHMMCE at rates ~30-fold less than those of the wild-type hMGL, whereas sol-S-hMGL hydrolyzed these substrates at rates ~2000-fold less than wild-type hMGL.

Inhibitor Profiles of Engineered hMGL Variants. Representatives of distinct classes of hMGL inhibitors (Figure 1) were profiled in both sol-hMGL and sol-S-hMGL. AM6580 and NAM are irreversible covalent inhibitors with distinct mechanisms: AM6580 is an irreversible inhibitor, whereas NAM is a sulfhydryl-modifying reagent that alkylates wild-type hMGL thiol groups (especially those of Cys^{208} and Cys^{242}).[18,20] AM10212 is a recently designed, reversible hMGL inhibitor.[21] After a 40 min enzyme preincubation period with inhibitor and as evaluated over 3 h in a kinetic assay, AM6580 inhibited sol-hMGL and sol-S-hMGL with equal potency (apparent IC_{50}'s of ~90 nM), likely reflecting in both cases enzyme inactivation consequent to rapid covalent modification by AM6580 (Table 2). Most strikingly, AM10212 was some 2000-fold more potent

Table 2. Apparent IC_{50} Values for Inhibition of Purified Recombinant sol-hMGL and sol-S-hMGL by AM6580, NAM, and AM10212

inhibitor	IC_{50} Sol-hMGL	IC_{50} sol-S-hMGL
AM6580	87 nM	88 nM
NAM	1.2 μM	5.8 μM
AM10212	5 nM[a]	10 μM[a]

[a]Derived from a concentration−response curve over a range of three AM10212 concentrations.

an inhibitor of sol-hMGL than of sol-S-hMGL (Table 2), suggesting a particularly critical role for Ser^{122} in the mechanism of hMGL inhibition by AM10212. The Ser^{122}-to-Cys substitution introduces an additional thiol site for potential interaction with NAM and might be expected to increase enzyme sensitivity to this alkylating reagent. However, the apparent NAM IC_{50} for sol-S-hMGL was ~5-fold higher than that for sol-hMGL (Table 1). Examination of the NAM concentration−response profiles of sol-hMGL and sol-S-hMGL (Figure 3), however, revealed that the activity of the sol-S-hMGL variant had already been reduced by ~25% upon fluorometric assay at the lowest NAM concentration tested (100 nM), indeed suggesting the existence of an additional, highly susceptible site for NAM alkylation in sol-S-hMGL.

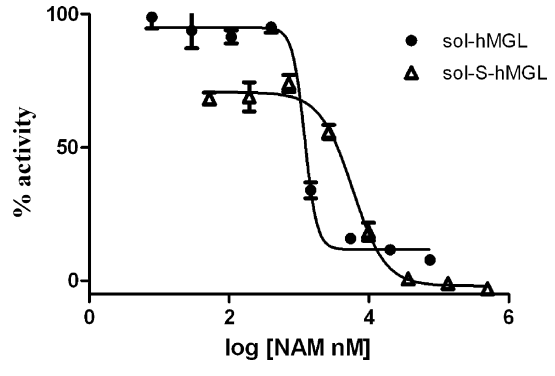

Figure 3. Concentration-dependent inhibition by NAM of AHMMCE hydrolysis by sol-hMGL (●) and sol-S-hMGL (△).

dx.doi.org/10.1021/cn3000263 | ACS Chem. Neurosci. 2012, 3, 393−399

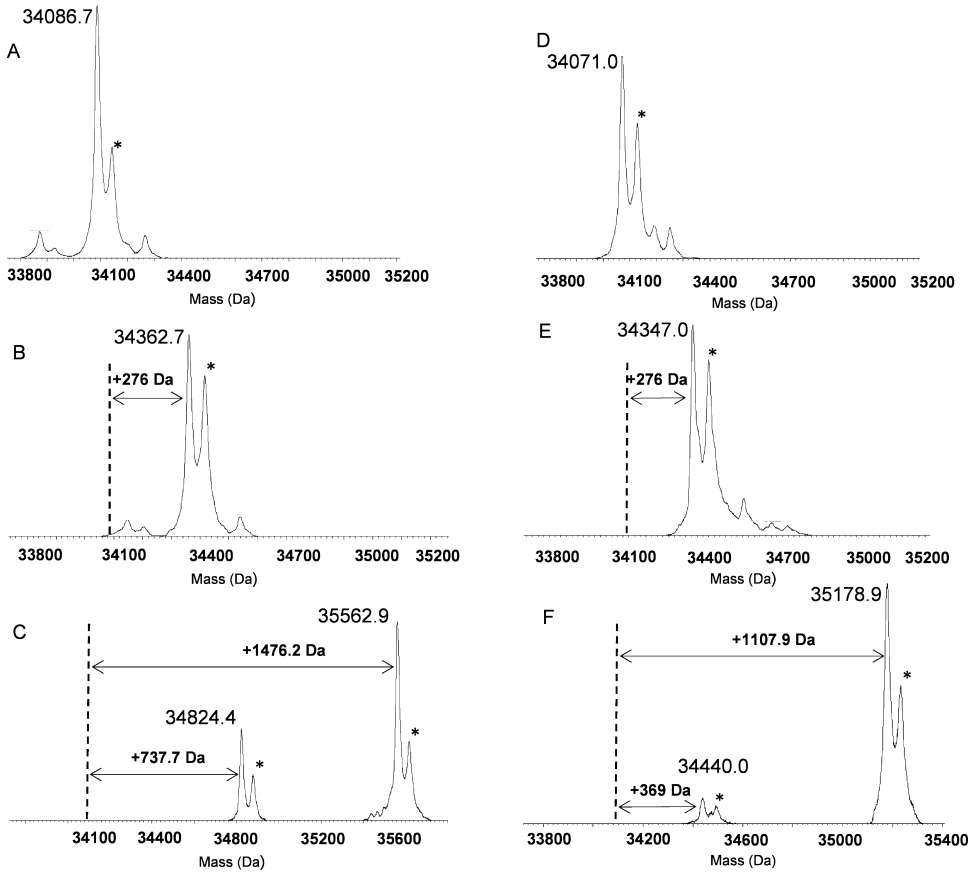

Figure 4. MS analysis of sol-S-hMGL and sol-hMGL enzyme masses. Intact masses of unmodified (A and D), AM6580-modified (B and E), and NAM-modified (C and F) sol-S-hMGL and sol-hMGL, respectively, analyzed with LCT Premier^{xe} MS instrument. (* denotes putative Fe^{2+}-6-His adduct.)

MS Analysis of sol-hMGL and sol-S-hMGL Inhibition by AM6580 and NAM. Samples of purified sol-hMGL and sol-S-hMGL were incubated for 40 min in buffer with a 4-fold molar excess of either AM10212, AM6580, or NAM in dimethyl sulfoxide (DMSO) or with DMSO vehicle only, after which incubation samples were desalted and analyzed by MS to determine the intact mass of each. The spectra of the inhibitor-free soluble hMGL variants each evidenced two prominent peaks with average massses 34 086.7 Da (calculated 34 086.8 Da) and 34 142.7 Da (+56 Da) for sol-S-hMGL and 34071.0 Da (calculated 34 070.7 Da) and 34 127.0 Da (+56 Da) for sol-hMGL (Figure 4A and D, respectively). A second, minor peak of variable intensity and +56 Da mass relative to enzyme was consistently observed across different preparations of these soluble hMGL variants that may reflect an Fe^{2+}-6-His protein adduct, given the Fe molecular weight of 56. The average intact masses of AM6580-treated sol-S-hMGL and sol-hMGL samples were 276.0 Da greater relative to the unmodified enzymes (Figure 4B and E, respectively), a result consistent with enzyme carbamoylation by AM6580 and the consequent calculated mass increase of 277.14 Da. The mass of either soluble hMGL variant did not change after incubation with the reversible inhibitor, AM10212 (data not shown).

Sol-hMGL and sol-S-hMGL contain four and five Cys residues, respectively, that could potentially be modified through NAM alkylation. Aside from the spurious +56 Da species referred to above, two enzyme species with average masses of 34 824.4 and 35 562.9 Da for sol-S-hMGL and 34 440.0 and 35 178.9 Da for sol-hMGL were observed in the MS analysis of each respective enzyme 40 min after enzyme incubation with a 4-fold molar excess of NAM (Figure 4C and F). Since NAM has an exact mass of 369.27, the average mass increase between untreated and NAM-treated sol-S-hMGL for each species [+737.7 Da (i.e., 34 824.4 minus 34 086.7) and +1476.2 Da (i.e., 35 562.9 minus 34 086.7)] indicates that both sol-S-hMGL species could be alkylated by NAM at two and four of the available cysteines, respectively (Figure 4C). The mass increases after incubation with NAM for the two major sol-hMGL species [+369 Da (i.e., 34 440 minus 34 071) and +1107.9 Da (i.e., 35 178.9 minus 34 071)] indicate that either one or three of their Cys residues had been alkylated by NAM. Markedly less intense signals indicative of sol-hMGL modified by two NAM molecules and sol-S-hMGL modified by one or three NAM molecules were also observed (data not shown). These results for the sol-hMGL variant are congruent with our prior MS analysis showing that, of the four Cys residues in wild-type NAM, only three are alkylated maximally, even in the presence of a large molar excess of NAM over enzyme.[18] Thus, the fourth Cys alkylated by NAM in sol-S-hMGL is likely the Cys^{122} introduced into the catalytic site of sol-hMGL.

Desalted samples of sol-S-hMGL incubated without inhibitor or with either AM6580 or NAM were digested with trypsin, and the tryptic digests were analyzed by LC/MS. The tryptic peptide of inhibitor-free sol-S-hMGL that contains the Ser^{122}-to Cys mutation appears as ion m/z 1053.49 for charge state +5 (1053.49 Da × 5 − 5 Da = 5262.45 Da; calculated 5262.75 Da) (Figure 5A). The mass difference between the corresponding tryptic peptides from uninhibited and AM6580-treated sol-S-

dx.doi.org/10.1021/cn3000263 | ACS Chem. Neurosci. 2012, 3, 393−399

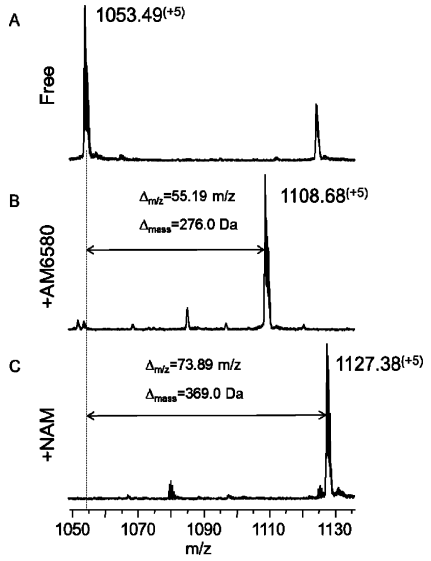

Figure 5. Tryptic peptide of sol-S-hMGL identified by MS^E and containing Cys^{122} of (A) unmodified enzyme; (B) enzyme modified with AM6580; (C) enzyme modified with NAM. The full hMGL sequence has been published in ref 17.

hMGL was 276.0 Da (1108.68 − 1053.49 Da = 55.19 Da × 5 = 276.0 Da; calculated increase due to carbamoylation, 277.14 Da), consistent with covalent sol-S-hMGL modification by AM6580 (Figure 5B). Four NAM-modified cysteines (at positions 122, 201, 208, and 242), were identified in the tryptic digests of sol-S-hMGL. Cys^{201}, Cys^{208}, and Cys^{242} showed evidence for both modified and unmodified peptides, whereas Cys^{32} remained unmodified (data not shown). The tryptic peptide of NAM-treated sol-S-hMGL containing the catalytic Ser^{122}-to-Cys substitution appears as ion m/z 1127.38 for charge state +5, corresponding to a mass increase of 369.45 Da (73.89 Da × 5 = 369.45 Da). This mass increase is consistent with alkylation by NAM, which has a mass of 369.27 (Figure 5C). These collective data show that the nucleophilic residue in the hMGL catalytic triad of sol-hMGL and sol-S-hMGL is covalently modified: Ser^{122} is carbamoylated and Cys^{122} thiocarbamoylated by AM6580, and Cys^{122} is alkylated by NAM.

In conclusion, we have successfully engineered two soluble hMGL variants whose demonstrated catalytic competency allowed us to interrogate and define the enzyme's distinctive interaction profiles with three inhibitors of differing chemical reactivities. Substitution of the sol-hMGL catalytic-triad Ser^{122} with an alternative nucleophile, Cys, reduced hMGL nucleophilic catalysis without apparently compromising enzyme structural integrity. Our results suggest that the 3D architecture of hMGL as a serine esterase is optimized to take particular advantage of the nucleophilicity of its activated, active-site Ser^{122} residue. This enhanced reactivity is not fully actualized when Ser^{122} is substituted with the generally more nucleophilic Cys. The data thus demonstrate the importance of the activated Ser^{122} for optimal hMGL catalytic activity and suggest that, in the context of the hMGL enzyme, the active-site Ser^{122} is a more potent nucleophile than is Cys^{122}. The effect of the Ser^{122}-to-Cys substitution is most striking when the noncovalent, reversible inhibitor, AM10212, is used, underscoring the dominant role of the catalytic Ser^{122} residue on enzyme−ligand equilibrium when compared to that of Cys^{122}. We are currently exploring the structural features of this hMGL−ligand interaction using high-resolution NMR. Given recent preclinical evidence that the biological effects of NAM inhibition can vary markedly with the duration of pharmacological NAM inhibition,[4,22] our MS data support the proposition that the temporal tuning of small-molecule hMGL inhibitors may require distinct modes of interaction with the enzyme in order for such agents to be considered viable therapeutic candidates.

METHODS

Materials. Standard laboratory chemicals, culture media, isopropyl-β-D-thio-galactopyranoside, lysozyme, and DNase I were purchased from Sigma Chemical Co. (St. Louis, MO) and Fisher Chemical (Pittsburgh, PA), unless otherwise specified. Electrophoresis supplies were from Bio-Rad (Hercules, CA). MS-grade trypsin (Trypsin Gold) was from Promega (Madison, WI). AM6580, AM10212, and AHMMCE were synthesized at the Center for Drug Discovery, Northeastern University, by standard routes specified elsewhere.[18,20,21] NAM was purchased from Cayman Chemical (Ann Arbor, MI).

Mutant hMGL Preparation, Expression, and Purification. The Leu(Leu^{169};Leu^{176})-to-Ser(Ser^{169};Ser^{176}) hMGL double mutant (sol-hMGL) and the Ser^{122}-to-Cys sol-hMGL triple mutant (sol-S-hMGL) were generated as 6-His-tagged proteins using the QuickChange site-directed mutagenesis kit (Agilent-Stratagene, La Jolla, CA). The DNA primary structure of the mutants was confirmed by sequencing. All hMGL mutants were expressed in *E. coli* essentially as previously detailed.[17,18] In brief, a single *E. coli* BL21 (DE3) colony containing the plasmids with appropriate mutations in hMGL gene was inoculated into 10 mL of Luria broth supplemented with ampicillin (100 μg/mL) and grown overnight at 30 °C with shaking (250 rpm). The next morning, these 10 mL cultures were used to inoculate 500 mL of fresh Luria broth-ampicillin medium and allowed to grow under the specified conditions until the culture reached an OD_{600} of 0.6−0.8, at which time expression was induced by adding 0.4 mM (final concentration) isopropyl-β-D-thiogalactopyranoside. After 4 h induction, the cells were harvested by centrifugation, washed with phosphate-buffered saline, and held at −80 °C. Three grams (wet-weight) of cells were resuspended in 20 mL of lysis buffer [20 mM Na-phosphate, pH 7.45, containing 150 mM NaCl] and 20 mL xTractor buffer and disrupted on ice by six, 30 s sonication cycles, each cycle consisting of 1 s bursts at 50 W separated by a 5 s interval. The resulting lysate, after centrifugation (20 000*g*, 25 min, 4 °C), was used for hMGL purification through an immobilized metal-affinity chromatography-based procedure to be detailed elsewhere. Functional, monomeric hMGL variants were obtained, the purity of which was checked under denaturing conditions on SDS-PAGE gels. Proteins were stained with Commassie blue and photographed with a FluorChem imaging system (Alpha Innotech, San Leandro, CA). Prior to enzyme assay, hMGL samples in elution buffer (20 mM Na-phosphate, pH 7.45, containing 150 mM NaCl and 300 mM imidazole) were dialyzed for 12 h to ensure thorough imidazole removal using a membrane with a molecular-weight cutoff of 12 000−14 000 Da. Enzyme protein concentration was determined spectrophotometrically using the molar extinction coefficient ε_{280} = 24 910 M^{-1} cm^{-1}.

hMGL Assay. hMGL activity was assessed by two methods. In the first, hydrolysis of 2-AG to arachidonic acid (AA) was quantified by HPLC.[23] Briefly, 2-AG at varying concentrations from 13 to 400 μM and either sol-hMGL (18 ng) or sol-S-hMGL (3.2 μg) in TME buffer (300 μL, total vol) were incubated at 37 °C. Reaction samples (50 μL) were taken immediately at the start of the incubation and after 20 min, diluted 1:4 (v/v) with acetonitrile, and centrifuged at 20 000*g* for 5 min at room temperature. A 10 μL aliquot of supernatant was injected onto the C18 HPLC column (4.6 × 50 nm; Zorbax, Agilent) with chromatographic conditions previously detailed.[17] In an 8 min run, 2-AG eluted at 3.0 min, and AA at 6.0 min, allowing the reaction to be followed by either substrate (2-AG) conversion or product (AA) formation. Analytes were quantified with external standards.

In the second, hMGL activity was measured as the hydrolysis of the reporter fluorogenic substrate, AHMMCE, to coumarin fluorophore, essentially as developed and detailed previously by us.[17] AHMMCE was stored at −20 °C as a 10 mM DMSO stock solution, which was thawed and diluted 1:1 (v/v) with assay buffer (50 mM Tris-HCl, pH 7.4) such that the final DMSO concentration in each assay reaction was well below 8% to ensure that the AHMMCE remained in solution during the assay. To start the enzyme reaction, AHMMCE from the diluted stock was added to a known amount of either sol-hMGL or sol-S-hMGL protein to achieve a final substrate concentration of 100 μM in a total assay volume of 200 μL. Reactions were incubated at 22 °C, and fluorescence readings at 360 nm/460 nm ($\lambda_{excitation}/\lambda_{emission}$) were taken every 15 min over a 3 h period with a Synergy HT plate reader (BioTek Instruments, Winooski, VT) in kinetic mode. Relative fluorescence units were converted to the amount of coumarin formed based on a coumarin standard curve. Under these conditions, nonenzymatic AHMMCE hydrolysis to coumarin was negligible.

Intact Mass Determination and Tryptic Digest Analysis of hMGL Variants Treated with AM6580 and NAM. Purified sol-hMGL or sol-S-hMGL (400 μM each) in 30 μL of 20 mM Na-phosphate buffer, pH 7.45, containing 150 mM NaCl was incubated for 1 h at room temperature in the absence or presence of either AM6580 or NAM at 4-fold molar excess with respect to enzyme. After evaluation of enzyme inhibition with AM6580 or NAM by the fluorescence assay, excess inhibitor was removed by desalting with a Bio-Spin 6 column in the same buffer. Samples were then taken for intact mass determination and trypsin digestion at 35 °C.

For intact mass determination, 40 μg of hMGL was injected onto a self-packed POROS 20 R2 protein trap (Applied Biosystems) and desalted with 1.0 mL of 0.05% aqueous TFA at a flow rate of 500 μL/min. Protein was eluted into the mass spectrometer using a linear 15−75% acetonitrile gradient over 4 min at 50 μL/min and a Shimadzu LC (LC-10ADvp). Mass spectral analyses were carried out with a Waters LCT-Premier^{XE} mass spectrometer under conditions of a standard electrospray source, a capillary voltage of 3.0 kV, and a cone voltage of 35 V.

Desalted sol-S-hMGL samples were digested with MS-grade trypsin (hMGL/trypsin ratio, 1:200) overnight at 35 °C. Each aliquot of tryptic digest (3 μL, 1.2 nmol protein) was diluted into 50 μL of 0.1% aqueous formic acid prior to injection onto a custom Waters nanoACQUITY UPLC for online desalting and reverse-phase separation. Tryptic peptides were trapped and desalted on a VanGuard Pre-Column (2.1 mm × 5 mm, ACQUITY UPLC BEH C18, 1.7 μm) for 3 min at 100 μL/min. The trap was placed in-line with an ACQUITY UPLC BEH C18 1.7 μm 1.0 × 100 mm column (Waters), and peptides were eluted into the mass spectrometer with a 5−40% gradient of acetonitrile over 92 min at a flow rate of 40 μL/min. All mobile phases contained 0.1% formic acid, and the temperature of all components was 21 °C. Mass spectral analysis was carried out on a Waters Q-TOF Premier instrument with settings as follows: 3.5 kV cone and 35 V capillary voltages; source and desolvation temperatures 80 and 175 °C, respectively; desolvation gas flow of 600 L/h. All mass spectral data were collected in triplicate in ESI (+), V mode, and MS^{E} mode over the m/z range 50−1700. Peptides produced from overnight trypsin digestion were identified using Waters ProteinLynx Global Server version 2.5 with Identity Informatics software.

AUTHOR INFORMATION

Corresponding Author

*(D.R.J.) Mailing address: Northeastern University Center for Drug Discovery, 360 Huntington Avenue, Mugar 116, Boston, MA 02115-5555. Telephone: 617-373-2208. Fax: 617-373-7493. E-mail: d.janero@neu.edu. (A.M.) E-mail: a.makriyannis@neu.edu.

Author Contributions

All authors contributed equally to the manuscript.

Funding

This work was supported by National Institutes of Health/National Institute on Drug Abuse Grants DA 3801 and DA 9152.

Notes

The authors declare no competing financial interest.

ACKNOWLEDGMENTS

The expert technical advice of Dr. JodiAnne T. Wood is gratefully appreciated.

ABBREVIATIONS

MGL, monoacylglycerol lipase; 2-AG, 2-arachidonoylglycerol; CB1R, cannabinoid-1 receptor; CB2R, cannabinoid-2 receptor; hMGL, human monoacylglycerol lipase; sol-hMGL, Leu-(Leu^{169};Leu^{176})-to-Ser(Ser^{169}/Ser^{176}) 2 L/2S double hMGL mutant; sol-S-hMGL, Leu(Leu^{169};Leu^{176})-to-Ser(Ser^{169}/Ser^{176}) and Ser^{122}-to-Cys triple hMGL mutant; NAM, *N*-arachidonylmaleimide; AM6580, [4-(9H-fluoren-9-yl)piperazin-1-yl]-[1,2,3]triazolo[4,5-b]pyridin-1-ylmethanone; AM10212, 2-cyclohexyl-6-{[3-(4-pyrimidin-2-yl-piperazin-1-yl)azetidin-1-yl]-carbonyl}-1,3-benzoxazole; AHMMCE, arachidonoyl, 7-hydroxy-6-methoxy-4-methylcoumarin ester; CNS, central nervous system; MS, mass spectroscopy; DMSO, dimethyl sulfoxide; AA, arachidonic acid

REFERENCES

(1) Di Marzo, V. (2009) The endocannabinoid system: its general strategy of action, tolls for its pharmacological manipulation and potential therapeutic exploitation. *Pharamcol. Res. 60* (2), 77−84.

(2) Blankman, J. L., Simon, G. M., and Cravatt, B. F. (2007) A comprehensive profile of brain enzymes that hydrolyze the endocannabinoid 2-arachidonoylglycerol. *Chem. Biol. 14* (12), 1347−1356.

(3) Long, J. Z., Li, W., Booker, L., Burston, J. J., Kinsey, S. G., Schlosburg, J. E., Pavón, F. J., Serrano, A. M., Selley, D. E., Parsons, L. H., Lichtman, A. H., and Cravatt, B. F. (2009) Selective blockade of 2-arachidonoylglycerol hydrolysis produces cannabinoid behavioral effects. *Nat. Chem. Biol. 5* (1), 37−44.

(4) Schlosburg, J. E., Blankman, J. L., Long, J. Z., Nomura, D. K., Pan, B., Kinsey, S. G., Nguyen, P. T., Ramesh, D., Booker, L., Burston, J. J., Thomas, E. A., Selley, D. E., Sim-Selley, L. J., Liu, Q. S., Lichtman, A. H., and Cravatt, B. F. (2010) Chronic monoacylglycerol lipase blockade causes functional antagonism of the endocannabinoid system. *Nat. Neurosci. 13* (9), 1113−1119.

(5) Chanda, P. K., Gao, Y., Mark, L., Btesh, J., Strassle, B. W., Lu, P., Piesla, M. J., Zhang, M. Y., Bingham, B., Uveges, A., Kowal, D., Garbe, D., Kouranova, E. V., Ring, R. H., Bates, B., Pangalos, M. N., Kennedy, J. D., Whiteside, G. T., and Samad, T. A. (2010) Monoacylglycerol lipase activity is a critical modulator of the tone and integrity of the endocannabinoid system. *Mol. Pharmacol. 78* (6), 996−1003.

(6) Pan, B., Wang, W., Zhong, P., Blankman, J. L., Cravatt, B. F., and Liu, Q. S. (2011) Alterations of endocannabinoid signaling, synaptic plasticity, learning, and memory in monoacylglycerol lipase knock-out mice. *J. Neurosci. 31* (38), 13420−13430.

(7) Nomura, D. K., Morrison, B. E., Blankman, J. L., Long, J. Z., Kinsey, S. G., Marcondes, M. C., Ward, A. M., Hahn, Y. K., Lichtman, A. H., Conti, B, and Cravatt, B. F. (2011) Endocannabinoid hydrolysis generates brain prostaglandins that promote neuroinflammation. *Science 334* (6057), 809−813.

(8) Nomura, D. K., Long, J. Z., Niessen, S., Hoover, H. S., Ng, S.-W., and Cravatt, B. F. (2010) Monoacylglycerol lipase regulates a fatty acid network that promotes cancer pathogenesis. *Cell 140* (1), 49−61.

(9) Nomura, D. K., Lombardi, D. P., Chang, J. W., Niessen, S., Ward, A. M., Long, J. Z., Hoover, H H., and Cravatt, B. F. (2011) Monoacylglycerol lipase exerts dual control over endocannabinoid and

fatty acid pathways to support prostate cancer. *Chem. Biol. 18* (7), 846−856.
(10) Kinsey, S. G., Long, J. Z., O'Neal, S. T., Abdullah, R. A., Poklis, J. L., Boger, D. L., Cravatt, B. F., and Lichtman, A. H. (2009) Blockade of endocannabinoid-degrading enzymes attenuates neuropathic pain. *J. Pharmacol. Exp. Ther. 330* (3), 902−910.
(11) Long, J. Z., and Cravatt, B. F. (2011) The metabolic serine hydrolases and their functions in mammalian physiology and disease. *Chem. Rev. 111* (10), 6022−6063.
(12) Bachovchin, D. A., and Cravatt, B. F. (2012) The pharmacological landscape and therapeutic potential of serine hydrolases. *Nat. Rev. Drug Discovery 11* (1), 52−68.
(13) Bertrand, T., Auge, F., Houtmann, J., Rak, A., Vallee, F., Mikol, V., Berne, P. F., Michot, N., Cheuret, D., Hoornaert, C., and Mathieu, M. (2010) Structural basis for human monoglyceride lipase inhibition. *J. Mol. Biol. 396* (3), 663−673.
(14) Labar, G., Bauvois, C., Borel, F., Ferrer, J. L., Wouters, J., and Lambert, D. M. (2010) Crystal structure of the human monoacylglycerol lipase, a key actor in endocannabinoid signaling. *Chem. Biochem. 11* (2), 218−227.
(15) Schalk-Hihi, C., Schubert, C., Alexander, R., Bayoumy, S., Clemente, J. C., Deckman, I., DesJarlais, R. L., Dzordzorme, K. C., Flores, C. M., Grasberger, B., Kranz, J. K., Lewandowski, F., Liu, L., Ma, H., Maguire, D., Macielag, M. J., McDonnell, M. E., Haarlander, T. M., Miller, R., Milligan, C., Reynolds, C., and Kuo, L. C. (2011) Crystal structure of a soluble form of human monoglyceride lipase in complex with an inhibitor at 1.35 A resolution. *Protein Sci. 20* (4), 670−683.
(16) Karlsson, M., Contreras, J. A., Hellman, U., Tornqvist, H., and Holm, C. (1997) cDNA cloning, tissue distribution, and identification of the catalytic triad of monoglyceride lipase. *J. Biol. Chem. 272* (43), 27218−27223.
(17) Zvonok, N., Williams, J., Johnston, M., Pandarinathan, L., Janero, D. R., Jing, L. I., Krishnan, S. C., and Makriyannis, A. (2008) Full mass spectrometric characterization of human monoacylglycerol lipase generated by large-scale expression and single-step purification. *J. Proteome Res. 7* (5), 2158−2164.
(18) Zvonok, N., Pandarinathan, L., Williams, J., Johnston, M., Karageorgos, I., Janero, D. R., Krishnan, S. C., and Makriyannis, A. (2008) Covalent inhibitors of human monoacylglycerol lipase: ligand-assisted characterization of the catalytic site by mass spectrometry and mutational analysis. *Chem. Biol. 15* (8), 854−862.
(19) Karageorgos, I., Tyukhtenko, S., Zvonok, N., Janero, D. R, Sallum, C., and Makriyannis, A. (2010) Identification by nuclear magnetic resonance spectroscopy of an active-site hydrogen-bond network in human monoacylglyerol lipase (hMGL): implications for hMGL dynamics, pharmacological inhibition, and catalytic mechanism. *Mol. Biosyst. 6* (8), 1381−1388.
(20) Hoornaert, C. (2011) Triazolopyridine carboxamides derivatives, preparation thereof, and therapeutic uses thereof. Patent US7868007B2.
(21) Chevalier, K. M., Dax, S. L., Flores, C. M., Liu, L., Macielag, M. J., McDonnell, M. E., Nelen, M. I., Prouty, S., Todd, M., Zhang, S.-P., Zhu, B., Nulton, E. L., and Clemente, J.(2010) Heteroaromatic and aromatic piperazinyl azetidinyl amides as monoacylglycerol lipase (MGL) inhibitors. Patent WO2010124121A1.
(22) Lichtman, A. H., Blankman, J. L., and Cravatt, B. F. (2010) Endocannabinoid overload. *Mol. Pharmacol. 78* (6), 993−995.
(23) Lang, W., Qin, C., Hill, W. A., Lin, S., Khanolkar, A. D., and Makriyannis, A. (1996) High-performance liquid chromatographic determination of anandamide amidase activity in rat brain microsomes. *Anal. Biochem. 238* (1), 40−45.